Original Research Article

Dexmedetomidine alleviates microglial activation of neuropathic pain by modulating miR-23a /PDE10A axis in streptozotocin-induced diabetic mice

Qian Wu[1], Yan Qiao[2], Jiannan Song[3]*
[1]Health Management Center, Wuhan Third Hospital, Wuhan City, Hubei Province, 430074, [2]Department of Neurology, 024000, [3]Department of Anesthesiology, Chifeng Municipal Hospital, Chifeng City, Inner Mongolia Autonomous Region 024000, China

*For correspondence: **Email:** songjiannan321@163.com; **Tel:** +86-0476-8365914

Abstract

Purpose: To elaborate the functional role of dexmedetomidine (DEX) in alleviating microglial activation of diabetic neuropathic pain (DNP) and explore the involved signaling pathways.
Methods: The viability of BV-2 cells was measured using a commercial kit. Levels of interleukin 1β (IL-1β) and tumor necrosis factor-α (TNF-α) were measured using commercial ELISA kit. The mRNA target was predicted and confirmed using TargetScan and luciferase assay. Protein expression levels were determined by western blotting. Diabetes was indiced in C57BL/6J mice using streptozotocin (STZ) and antidiabetic parameters evaluated in vivo.
Results: DEX suppressed HG-induced microglial activation in BV-2 cells. The levels of IL-1β and TNF-α increased in HG-treated cells, but this was counteracted following DEX treatment. Phosphorylation of p65 (p-p65) was upregulated in cells treated with HG, while DEX repressed this upregulation. MiR-23a was downregulated in BV-2 cells treated with HG, but upregulated by addition of DEX. MiR-23a mimics repressed the induction of IL-1β and TNF-α levels and expression of p-p65. Results from TargetScan and luciferase assays showed that the 3-untranslated region (UTR) of PDE10A was directly targeted by miR-23a. The in vivo studies showed that miR-23a agomir relieved neuropathic pain and reduced the expressions of PDE10A and p-p65 in STZ-induced diabetic mice, but these effects were aggravated by DEX.
Conclusion: The results show that upregulation of miR-23a, DEX alleviates microglial activation of neuropathic pain and reduces levels of inflammatory factors in STZ-induced diabetic C57BL/6J mice. The underlying mechanism was at least partially mediated by PDE10A.

Keywords: Dexmedetomidine, Microglial activation, Diabetic neuropathic pain, MiR-23a, PDE10A

INTRODUCTION

Diabetic neuropathic pain (DNP), one of the most difficult types of pain, is considered as a most occurred microvascular complication of diabetes mellitus (DM), which significantly reduces life quality of DM patients [1]. The management of DNP consists of reducing the levels of fasting blood glucose [1]. However, the pathological mechanism of DNP is still not completely clear.

Current treatments for DNP can cause side effects and drug resistance [1]. Thus, it is necessary to explore the mechanism by which DNP occurs and discover new and effective medications.

As a class of noncoding RNAs (18–22 nucleotides in length) [2], miRNAs act as gene suppressors, inhibiting expression of target mRNAs by targeting the 3'-untranslated regions (UTRs) [3]. Results of microarray analyses have revealed the alterations in the miRNAs expressions in streptozotocin (STZ)-induced DM mice, indicating that the abnormal miRNA expression profiling in DM progression [4]. Another study revealed that level of serum miR-23a, a biomarker of pre-diabetes with normal glucose tolerance, was reduced in type 2 DM[5]. Phosphodiesterase 10A (PDE10A), an 89-kDa dual-specific phosphodiesterase, catalyzes the breakdown of cAMP and cGMP and is mainly expressed in the mammalian striatum [6]. PDE10A has been reported associated with diabetes and neurological disorders [7]. However, there are no publications considering the relationship between PDE10A expression and progression and development of DNP.

Dexmedetomidine (DEX), a widely-used selective α2-adrenergic agonist, is applied in surgical sedation with no respiratory depression [8]. Previous studies have reported that DEX attenuates neuropathic pain [9]. For example, in a rat model, DEX ameliorated chronic constriction injury-induced neuropathic pain by inhibiting the JAK/STAT signaling pathway [10] and by reducing purinergic receptor 7 expression and extracellular signal-regulated kinase phosphorylation [11]. This present article is to elaborate the functional effects of DEX on alleviating DNP and identify the involved signaling pathways in this pathological process, which will identify new treatments for DNP.

EXPERIMENTAL

Reagents

BV-2 cells and HEK293 cells were purchased from ATCC (Manassas, VA, USA), penicillin/streptomycin were purchased from Sigma Aldrich (St. Louis, MO, USA), fetal bovine serum (FBS) was from Gibco (Grand Island, NY, USA), D-glucose was from GuideChem, China, miR-23a mimics, miR-23a inhibitors, and their corresponding negative controls (NC mimics and NC inhibitor) were purchased from RiboBio (Guangzhou, China). Lipofectamine 2000, TRIzol reagent was from Invitrogen (Carlsbad, CA, USA). CCK-8 reagent was from Beyotime

(Jiangsu, China), multiplate reader was from BioTek Epoch (Winooski, VT, USA).

PrimeScript™ RT Reagent Kit was from Takara (Dalian, China), KAPA SYBR® FAST qPCR Kit Master Mix (2X) Universal was from Applied Biosystems (Foster City, CA, USA), ELISA assays were all from R&D System (Minneapolis, MN, USA), psiCHECK2 vector and the dual luciferase reporter assay kit were from Promega (Madison, WI, USA), PVDF membranes were from Merck KGaA (Darmstadt, Germany), extraction buffers used for western blotting, and Pierce™ ECL Western Blotting Substrate was from (Thermo Fisher, USA), primary antibodies were from Abcam (Cambridge, MA, USA) or Cell Signaling Technology (Beverly, MA, USA). Male C57BL/6J mice were from Guangdong Medical Laboratory Animal Center (Guangdong Province, China).

Cell culture and various treatments

Murine microglial BV-2 cells and HEK293 cells were cultured in DMEM with supplements of 1% antibiotics including penicillin/streptomycin and FBS (10%) at 37 °C with 5% CO_2. BV-2 cells were cultured in sterile 6-well plates (1 × 10^5 cells/well) and treated with 100 mM of D-glucose for 24 h, named as high glucose (HG) group. Before HG treatment, BV-2 cells with pretreatment of 5, 10, and 20 μg/mL DEX were named as DEX-5 group, DEX-10 group and DEX-20 group.

Before treatment with HG, miR-23a mimics, inhibitors, and their corresponding negative controls were mixed with Lipofectamine 2000 and transfected into cells for 6 h.

CCK-8 assay

Cells were transferred into 96-well plates with 100 μL fresh media in each well and added with two microliters of CCK-8 reagent, followed by incubated for 2 h. The optical density (OD) value (450 nm) was read using a multiplate reader.

RNA extract and real-time quantitative PCR assay

Total RNA was isolated from cells or mouse tissues using the TRIzol reagent. The miR-23a expression was measured using the PrimeScript™ RT Reagent Kit and KAPA SYBR® FAST qPCR Kit Master Mix (2X) Universal. Relative expression of miR-23 was quantified using the $2^{-\Delta\Delta CT}$ method [12] with the listed primers (Table 1).

Table 1: Primers used in this study

Gene	Primer sequence (forward and reverse)
miR-23a	5'-ATCACATTGCCAGGGATT-3' 5'-CTCAACTGGTGTCGTGGA-3'
U6	5'-ATGGGTCGAAGTCGTAGCC-3' 5'-TTCTCGGCGTCTTCTTTCTCG-3'

ELISA

TNF-α and IL-1β were detected using the mouse TNF-α Quantikine ELISA Kit and mouse IL-1β/IL-1F2 Quantikine ELISA Kit, respectively.

Luciferase assay

The WT (wild-type) and MUT (mutant) sequences of 3'-UTR of PDE10A, which contains the putative binding site of miR-23a, were cloned into the psiCHECK2 vector, which named as psiCHECK2-PDE10A-WT and psiCHECK2-PDE10A-MUT plasmids, respectively. The constructed plasmids were then co-transfected with miR-23a mimics, miR-23a inhibitor, or the corresponding controls into HEK293 cells, and the luciferase activity was finally determined.

Western blotting

The cultured cells and tissues were lysed and proteins were separated by SDS-PAGE and transferred onto PVDF membranes and blocked with fat-free milk (5%). The membranes were then probed using primary antibodies (4 °C, overnight) and then incubated with secondary antibodies (2 h, room temperature). The protein signals were detected using the ECL system. The used primary antibodies were PDE10A (ab151454, 1:1,000 dilution); phospho-p65 (CST#3033, 1:1,000 dilution); p65 (CST#9460, 1:1,500 dilution), and β-actin (CST#3700, 1:3,000 dilution).

Animal model

Male C57BL/6J mice (15 weeks old) were housed (23 ± 2 °C, 55 ± 15 % humidity, 12 h light/12 h dark cycle) for 1 week and fed with normal mouse chow and water. All experiments were approved by the Ethics Committee of Chifeng Municipal Hospital (approval no. 2020-026) and performed in compliance with the Care and Use of Laboratory Animals published by the U.S. National Institutes of Health (no. 85-23, 1996) [13].

STZ (200 mg/kg) was used to induce diabetes, and DEX (2.5 μg in 20 μL normal saline for each mouse) was used to relieve neuropathic pain. The mice were grouped (n = 10 mice/group).

Sham group, mice were injected intraperitoneally (i.p.) with 20 μL normal saline. STZ group, mice were injected (i.p.) with STZ once. STZ + DEX group, mice were injected (i.p.) with STZ once. After 28 days, mice were intrathecally (i.t.) injected with DEX once daily for three days. STZ + NC agomir group, mice were injected (i.p.) with STZ once. After 28 days, mice were administered the negative control of miR-23a agomir (100 ng) by tail vein injection once daily for one week. STZ + miR-23a agomir group, mice were injected (i.p.) with STZ once. After 28 days, mice were then administered the miR-23a agomir (100 ng) by tail vein injection once daily for one week. STZ + miR-23a agomir + DEX group, mice were injected i.p. with STZ once and then administered the miR-23a agomir (100 ng) by tail vein injection once daily for one week. After that, mice were injected i.t. with DEX once daily for three days. After treatment, mouse body weights were measured. Blood glucose levels of mice were measured via tail vein.

Assessment of mechanical paw withdrawal threshold (MPWT)

The von Frey filament stimulation was used to test for MPWT. Mice were kept in a cage with a wire mesh floor for 30 min to acclimate to the environment. The plantar surface of their hind paws was stimulated with a calibrated series of von Frey hairs in ascending order (0.2 0.4, 0.6, 0.8, 1, 1.4, 2, 4, 6, and 8 g) for 6 sec per filament. The lowest amount of force required to elicit a response was regarded as MPWT.

Immunofluorescent staining

After treatment, mice were anesthetized using pentobarbital (i.p., 80 mg/kg). After collection of lumbar spinal tissues, which were then fixed in paraformaldehyde (4%, 4 °C, overnight) and cryopreserved in sucrose (30%). The spinal cords were incubated with ionized calcium-binding adaptor molecule 1 (IBA1) primary antibody (CST#17198, 1:300 dilution) at 4 °C overnight and then probed with anti-rabbit IgG (Alexa Fluor® 594 Conjugate) (CST#8889, 1:1,000 dilution). Fluorescence intensity was observed and photographed using a Leica TCS SPE confocal microscope.

Statistical analysis

Statistical analysis on data was performed using GraphPad Prism 7.8 software. The Student's *t* test, and one-way and two-way analyses of variance were used to analyze differences between two groups, and among three or more

groups, respectively. *P* < 0.05 was considered statistically significant.

RESULTS

DEX reduces HG-induced microglial activation in BV-2 cells

The different concentrations of DEX cause no significant changes in the activity of HG-treated BV-2 cells as compared to that treatment with HG alone (Figure 1 A). The levels of both IL-1β and TNF-α were induced by HG treatment (Figure 1 B). However, the level of TNF-α was significantly reduced by 10 and 20 µg/mL DEX, and the level of IL-1β was significantly reduced by 20 µg/mL DEX (Figure 1 B). The different concentrations of DEX cause no significant changes in the protein expression of p65 in HG-treated BV-2 cells as compared to that treatment with HG alone (Figure 1 C). The phosphorylation of p65 (p-p65) was increased by HG, but this phosphorylation was repressed by treatment with 10 and 20 µg/mL DEX (Figure 1 C). These data indicated that DEX reduced microglial activation induced by HG.
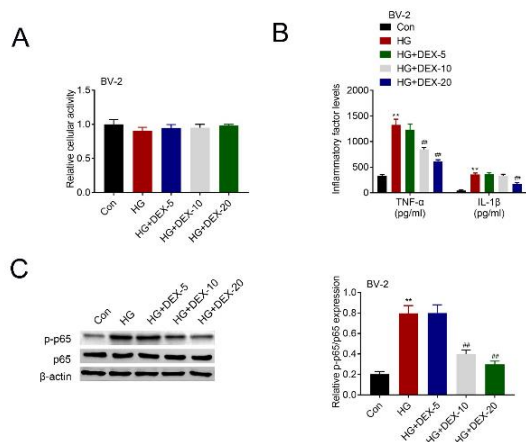
Figure 1: DEX suppresses HG-induced microglial activation in BV-2. The viability of HG-treated BV-2 cells (A), levels of IL-1β and TNF-α (B), and the protein expressions of p65 and p-p65 (C) after treatment with different concentrations of DEX. **P < 0.01 *vs.* Con; ##*P* < 0.01 *vs.* HG. DEX: dexmedetomidine; p-p65: phosphorylated p65.

DEX reverses HG-induced downregulation of miR-23a in BV-2 cells

The effects of DEX on miR-23a expression were measured. The miR-23a expression was inhibited in HG-treated BV-2 cells, which was increased in response to different concentrations of DEX, showing the highest expression at the concentration of 20 µg/mL (Figure 2).
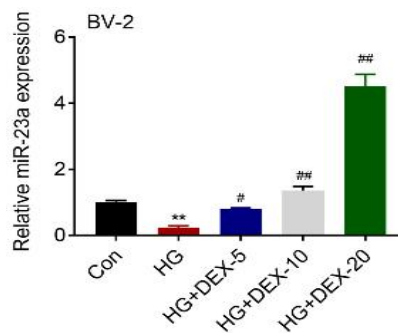
Figure 2: DEX reverses HG-induced downregulation of miR-23a in BV-2 cells. **P < 0.01 *vs.* Con; #*P* < 0.05 and ##*P* < 0.01 *vs.* HG. DEX: dexmedetomidine

MiR-23a mimic reduces HG-induced inflammation in BV-2 cells

The miR-23a expression was inhibited by HG, however, this inhibition was reversed in BV-2 cells after transfection of miR-23a mimic compared with that of NC mimics (Figure 3 A). The levels of IL-1β and TNF-α were increased by HG, but these inductions were prevented by miR-23a mimic (Figure 3 B). The protein expression of p-p65 was induced by HG, but inhibited by miR-23a mimic (Figure 3 C). These results suggested that miR-23a reduced HG-induced inflammation.
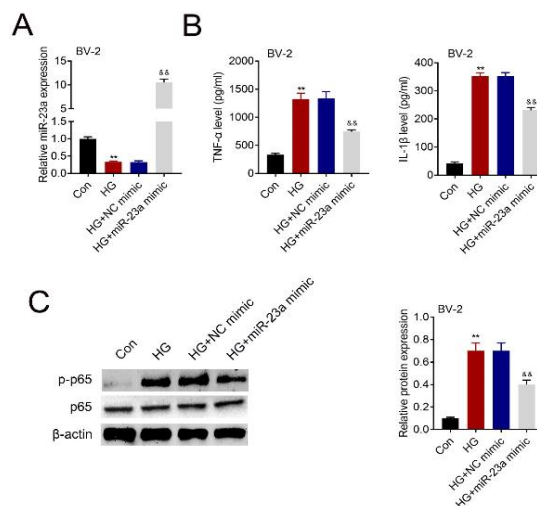
Figure 3: MiR-23a mimic reduces HG-induced inflammation in BV-2 cells. (A) Relative miR-23a expression in Con, HG, HG+NC mimic, and HG+miR-23a mimic groups. (B) IL-1β and TNF-α levels measured in BV-2 cells in different groups as described in (A). (C) Western blot analysis on the protein expression of p65 and p-p65 in BV-2 cells in different groups as described in (A). **P < 0.01 *vs.* NC mimic. &&*p* < 0.01 *vs.* NC inhibitor. NC mimic: negative control of miR-23a mimic

PDE10A is a direct target of miR-23a

TargetScan (www.tagetscan.org) predicted that there was a complementary sequence betwen miR-23a and the 3'-UTR of PDE10A (Figure 4 A). The luciferase activity was decreased by miR-23a mimic and enhanced by miR-23a inhibitor in the PDE10A-WT group as compared with the NC mimic and NC inhibitor (Figure 4 B). PDE10A protein expression was upregulated by miR-23a mimic and downregulated by miR-23a inhibitor (Figure 4 C). These results showed that PDE10A was directly targeted by miR-23a.
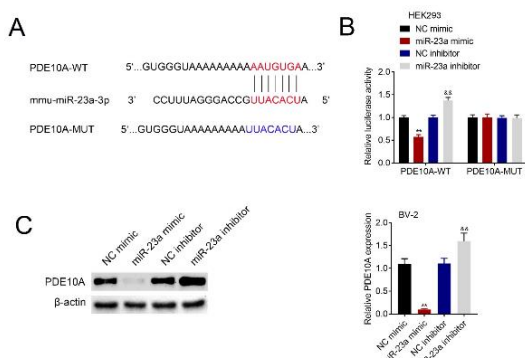
Figure 4: PDE10A is directly targeted by miR-23a. (A) The sequence between miR-23a-3p and its putative binding site in the 3′-UTR of PDE10A-WT. (B) Luciferase activity was measured in HEK293 cells. (C) PDE10A protein level was detected by western blot in BV-2 cells. **$P < 0.01$ *vs.* NC mimic; &&$p < 0.01$ *vs.* NC inhibitor. NC mimic: negative control of miR-23a mimic

DEX relieves DNP in STZ-induced DM mice via the miR-23a /PDE10A axis

The blood glucose level and body weight were increased after treatment with STZ in C57BL/6J mice (Figure 5 A). These inductions in blood glucose and body weights were not altered by either miR-23a agomir or the combination of miR-23a agomir and DEX (Figure 5 A). The mechanical allodynia and miR-23a expression were reduced by STZ, but these reductions were prevented by DEX (Figure 5 B and C). The protein expression of PDE10A and the p- p65, and the fluorescence intensity of IBA1 were significantly higher in STZ-treated mice as compared to that in Sham mice, but these inductions were prevented by DEX (Figure 5 D and E). Importantly, compared to that in STZ + NC agomir group, the mechanical allodynia and miR-23a expression was reduced, but the protein expressions of PDE10A and p-p65, and the fluorescence intensity of IBA1 were significantly increased in STZ + miR-23a agomir group (Figure 5 B and E). However, these alterations were aggravated by DEX treatment. These

investigations indicated that DEX relieved DNP in STZ-induced diabetic mice via the miR-23a.
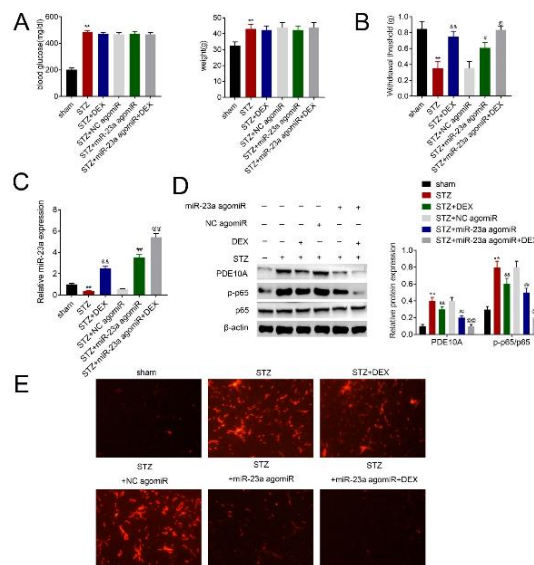
Figure 5: DEX relieves DNP in STZ-induced DM mice via the miR-23a /PDE10A axis. The blood glucose level and body weight (A), mechanical allodynia (B), miR-23a expression (C), protein expression of PDE10A and the p- p65 (D), and IBA1 fluorescence intensity (E) in C57BL/6J mice. **$P < 0.01$ *vs.* sham; &&$p < 0.01$ *vs.* STZ; #$p < 0.05$ and ##$p < 0.01$ *vs.* STZ + NC agomir; @$p < 0.05$ and @@$p < 0.01$ *vs.* STZ + miR-23a agomir. STZ: 200 mg/kg streptozotocin; NC agomir: negative control of the miR-23a agomir

DISCUSSION

As a selective α2-adrenergic agonist, DEX is widely used for surgical sedation [8]. It is also used to relieve pain, including postoperative pain, neuropathic pain, and chronic headache [9]. Our results demonstrated that the expression of miR-23a was reduced after treatment with HG. DEX reversed the HG-induced downregulation of miR-23a, alleviating DNP and reducing the productions of IL-1β and TNF-α via inhibiting the NF-κB signaling pathway. The underlying mechanism was mediated by downregulating PDE10A, a direct target of miR-23a.

DEX has been reported to relieve DNP via various inflammatory signals [14,15]. Consistently, DEX alleviated DNP in STZ-induced DM mice in the present study. Different mechanisms have been explored in previous studies, including by repression of P2X4 and NLR family pyrin domain containing 3 expression and downregulation of the Wnt 10a/β-catenin signaling pathway [14,15]. In this study, the HG-induced repression of miR-23a was attenuated by DEX via a different mechanism different from

previous conclusion. The *in vivo* experiments demonstrated that overexpression of miR-23a attenuated DNP, which was further attenuated by DEX treatment. These data suggest that the protective effects of DEX were mediated by upregulation of miR-23a.

IL-1β and TNF-α are pro-inflammatory cytokines that are induced during neuro-inflammation and contribute to pain hypersensitivity [16]. In this study, DEX and miR-23a mimic inhibited the production of IL-1β and TNF-α induced by HG, suggesting the anti-inflammatory effects of DEX and miR-23a. Microglia are the resident macrophages in the central nervous system and express many bioactive diffusible factors, including pro-inflammatory cytokines and neurotrophic factors that contribute to neuropathic pain [17]. IBA1 is a macrophage/microglia-specific calcium-binding protein that is specifically expressed in response to microglial activation during brain injury or disease [18]. Data from this study also showed that IBA1 expression is inhibited by DEX and miR-23 agomir, and further aggravated by the combination of DEX and the miR-23 agomir, indicating that DEX and miR-23a inhibit neuro-inflammation in microglia in STZ-induced diabetic mice.

NF-κB is a crucial transcription factor that regulates inflammation [19]. The p-p65, a component of NF-κB, activates inflammation via the NF-κB signaling pathway [19]. Here, the p-p65 was upregulated under diabetic conditions and was suppressed by DEX and miR-23a both *in vitro* and *in vivo*, suggesting that the relief of DNP by DEX treatment can be mediated by the inhibition of NF-κB signaling via the upregulation of miR-23a. In addition, the TargetScan results revealed a complementary sequence between the 3'-UTR of PDE10A and the "seed region" (2–8 nucleotides at the 5' end) of miR-23a. Luciferase activity was also decreased in cells co-transfection of miR-23a mimic and PDE10A-WT, confirming that PDE10A was directly targeted by miR-23a. Results of western blotting showed that PDE10A protein expression was downregulated by miR-23a mimics, further identifying PDE10A as a target of miR-23a.

CONCLUSION

The findings of the present study show that miR-23a is downregulated under HG conditions both in microglia and in mice, suggesting the identification of a new diagnostic biomarker for diabetes. DEX reverses the HG-induced downregulation of miR-23a, thus alleviating DNP by inhibiting of NF-κB signaling and reduction of

IL-1β and TNF-α production. These findings suggest a new therapeutic target for the treatment of DNP.

DECLARATIONS

Conflict of interest

No conflict of interest is associated with this work.

Contribution of authors

We declare that this work was performed by the authors named in this article, and all liabilities pertaining to claims relating to the content of this article will be borne by the authors. Qian Wu, Yan Qiao, and Jiannan Song designed the study, supervised the data collection, analyzed the data, interpreted the data, prepared the manuscript for publication, and reviewed the draft of the manuscript. All authors read and approved the manuscript.

Open Access

REFERENCES

1. *Lucarini E, Pagnotta E, Micheli L, Parisio C, Testai L, Martelli A, Calderone V, Matteo R, Lazzeri L, Di Cesare Mannelli L et al. Eruca sativa Meal against Diabetic Neuropathic Pain: An H(2)S-Mediated Effect of Glucoerucin. Molecules 2019; 24(16).*

2. *Qiu M, Shangguan Z, Zhang H. Downregulation of miR-451a in plasma may promote prothrombin expression and contribute to high blood coagulation state in gestational diabetes mellitus. Trop J Pharm Res 2020; 19(10): 2079-2084.*

3. *Liu X, Chen L, Liu Y, Zhang T. Tangeretin sensitises human lung cancer cells to TRAIL-induced apoptosis via ROS-JNK/ERK-CHOP pathway-mediated up-regulation of death receptor 5. Trop J Pharm Res 2017; 16(1): 17-29.*

4. *Gong Q, Lu Z, Huang Q, Ruan L, Chen J, Liang Y, Wang H, Yue Y, Feng S. Altered microRNAs expression profiling in mice with diabetic neuropathic pain. Biochem Biophys Res Commun 2015; 456(2): 615-620.*

5. Yang Z, Chen H, Si H, Li X, Ding X, Sheng Q, Chen P, Zhang H. Serum miR-23a, a potential biomarker for diagnosis of pre-diabetes and type 2 diabetes. Acta Diabetol 2014; 51(5): 823-831.

6. Whiteley EL, Tejeda GS, Baillie GS, Brandon NJ. PDE10A mutations help to unwrap the neurobiology of hyperkinetic disorders. Cell Signal 2019; 60(31-38.

7. Zagórska A. Phosphodiesterase 10 (PDE10) inhibitors: an updated patent review (2014-present). Expert Opin Ther Pat 2020; 30(2): 147-157.

8. Li A, Yuen VM, Goulay-Dufaÿ S, Sheng Y, Standing JF, Kwok PCL, Leung MKM, Leung AS, Wong ICK, Irwin MG. Pharmacokinetic and pharmacodynamic study of intranasal and intravenous dexmedetomidine. Br J Anaesth 2018; 120(5): 960-968.

9. Zhao Y, He J, Yu N, Jia C, Wang S. Mechanisms of Dexmedetomidine in Neuropathic Pain. Front Neurosci 2020; 14(330.

10. Xun S, Zheng R. Dexmedetomidine alleviates neuropathic pain by regulating JAK/STAT pathway in rats. J Cell Biochem 2020; 121(3): 2277-2283.

11. Lin JP, Chen CQ, Huang LE, Li NN, Yang Y, Zhu SM, Yao YX. Dexmedetomidine Attenuates Neuropathic Pain by Inhibiting P2X7R Expression and ERK Phosphorylation in Rats. Exp Neurobiol 2018; 27(4): 267-276.

12. Livak KJ, Schmittgen TD. Analysis of Relative Gene Expression Data Using Real-Time Quantitative PCR and the 2−ΔΔCT Method. Methods 2001; 25(4): 402-408.

13. Council NJP. Guide for the Care and Use of Laboratory Animals -- French Version. 1996; 327(3): 963-965.

14. Kang L, Yayi H, Fang Z, Bo Z, Zhongyuan X. Dexmedetomidine attenuates P2X4 and NLRP3 expression in the spine of rats with diabetic neuropathic pain. Acta Cir Bras 2019; 34(11): e201901105.

15. Zhong JM, Lu YC, Zhang J. Dexmedetomidine Reduces Diabetic Neuropathy Pain in Rats through the Wnt 10a/β-Catenin Signaling Pathway. Biomed Res Int 2018; 2018(9043628.

16. Li QY, Xu HY, Yang HJ. [Effect of proinflammatory factors TNF-α, IL-1β, IL-6 on neuropathic pain]. Zhongguo Zhong Yao Za Zhi 2017; 42(19): 3709-3712.

17. Tsuda M. Microglia in the spinal cord and neuropathic pain. J Diabetes Investig 2016; 7(1): 17-26.

18. Imai Y, Kohsaka S. Intracellular signaling in M-CSF-induced microglia activation: role of Iba1. Glia 2002; 40(2): 164-174.

19. Viatour P, Merville MP, Bours V, Chariot A. Phosphorylation of NF-kappaB and IkappaB proteins: implications in cancer and inflammation. Trends Biochem Sci 2005; 30(1): 43-52.